Development and Test of an High Power RF Plasma Thruster in Project SAPERE-STRONG

F. Trezzolani, M. Manente, A. Selmo and D. Melazzi
Technology for Propulsion and Innovation S.r.l., Padova, Italy

M. Magarotto, D. Moretto, P. de Carlo
Università degli Studi di Padova - CISAS "G. Colombo", Padova, Italy

M. Pessana
Thales Alenia Space, Italy

D. Pavarin
Università degli Studi di Padova - DII Dipartimento di Ingegneria Industriale, Padova, Italy

Abstract: The main objective of the project SAPERE/STRONG is the realization of a space tug, coupled to the rocket VEGA, devoted to the transfer of payloads of different sizes from an intermediate orbit to a target orbit. The principal propulsion system of the tug will be an Helicon Plasma Thruster; the University of Padova - CISAS "G. Colombo" is the partner responsible for the design, realization and testing of the mentioned thruster. We have developed two prototypes: i) a 200 W motor for preliminary testing with a target thrust of 8 mN for 0.4 mg/s Xe mass flow rate, ii) a 1 kW prototype, whose target thrust is roughly 100 mN, which is the real objective of the project. The principal instrumentation employed for the performances characterization is a thruster balance, developed within the same STRONG project, and a Faraday probe. The testing and optimization campaign is still ongoing at the CISAS facility, the preliminary results presented in this paper are related only to the 200 W prototype. We have described the balance measurement procedure using, as example, a 150 W input power and 0.2 mg/s Xe mass flow rate test: the measured thrust is $\mathbf{T = 1.43 \pm 0.18}$ mN. A performance characterization is available in the range: input power from 50 W up to 200 W, and the mass flow rate from 0.05 mg/s up to 0.2 mg/s; the thrust increases with both the input power and the mass flow rate, while the specific impulse decreases with the mass flow rate. A performances characterization in a wider range of input power and mass flow rate, and a performances optimization campaign have been scheduled for the next months.

I. Introduction

In the last years many efforts have been made to study and develop new plasma based propulsion systems, and nowadays these concepts are beginning to challenge the monopole of chemical thrusters in space propulsion. We can enumerate many advantages of plasma based systems in respect to traditional propulsion, some of them are: i) high specific impulse and in turn reduction of propellant mass, ii) high thrust efficiency. A peculiarity of plasma propulsion systems is the low thrust, therefore they have been employed in interplanetary missions[1] and in the position and attitude control systems of missions with high demanding requirements.[2] The majority of the missions in which a plasma propulsion system is employed rely on Ion Engines (IEs), and Hall Effect Thrusters (HETs). Both these concepts have been employed in space missions for decades and have proven to have good performances, but present some critical issues: i) limited life due to erosion of extracting grids or ceramic walls; ii) necessity of employing external cathodes in order to emit a plasma which is overall neutral.

In the past decade an innovative concept for space propulsion systems have been proposed: the Helicon Plasma Thruster[3] (HPT), whose plasma generation system is derived from high-density industrial plasma

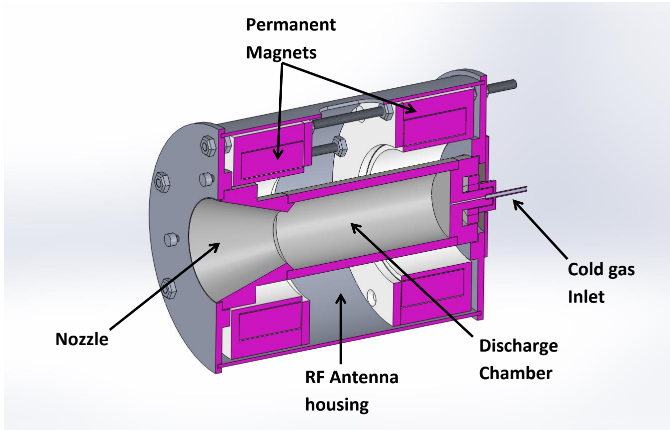

Figure 1. Helicon Plasma Thruster draft.

sources.[4] An HPT, see Figure 1, is mainly composed of a gas feeding system which provides the neutral propellant, a dielectric tube inside which the gas is ionized, an antenna working in the Radio Frequency (RF) regime (around some MHz) which produces the Electro Magnetic (EM) fields necessary to sustain the plasma, and coils or permanent magnets which creates a quasi-axial magneto-static field of hundreds of Gauss. The magneto-static field has three principal functions: i) confining the plasma, ii) allowing for the propagation of Helicon waves[5] which are the responsible of an efficient plasma generation, iii) creating a region in which the magnetic field lines are divergent at the exhaust of the source, providing a magnetic nozzle effect. In HPTs no electrodes in contact with the plasma nor neutralizers are employed, therefore HPTs are characterized by a long life. In addition HPTs have a good efficiency becouse of the magnetic field which reduces the heat losses.

HPTs are under study and development both in companies and research centers. The American "Ad Astra Rocket Company" have been involved for years in the VASIMR project,[6] where a high-power Helicon source is coupled to an ion cyclotron resonance heating section to increase the specific impulse; the VASIMIR rocket has been designed for working with a feeding power in the range of tents of kWs. The HPT technology has been widely studied in many academic research centers, at the University of Padova, in the frame of the European HPH.COM project[7,8] a low-power ($\leq$100 W) system has been developed. Other research centers which have developed HPTs prototypes are Australian National University,[9] Massachusetts Institute of Technology,[10] Tokyo University,[11] and Madrid University.[12]

Figure 2. The STRONG thruster prototype during a low power firing test with Ar propellant.

Nowadays at the University of Padova, Center for Space Studies and Activities CISAS "G. Colombo", the technology developed during the HPH.COM project is being employed within the Italian research project SAPERE.[13] The consortium of the SAPERE project is led by Thales Alenia Space Italia and involves CISAS as the partner responsible for the design, realization and testing of the electric propulsive system. SAPERE is organized in two sub-projects STRONG and SAFE. SAPERE/STRONG aims at the realization of a reusable space tug coupled to the rocket VEGA for the transfer of payloads of different sizes from an intermediate orbit to the target orbit. SAPERE/SAFE has as its primary purpose the improvement of "services for emergency management" (crisis management) in different domains, with a wider use of space technology in order to improve the possibility of observing from space, to communicate with space infrastructure, or to know the precise location. The electric propulsion system is an HPT with an input power of 1 kW, with a target thrust of roughly 100 mN, and capable of working with Xe, Ar and CO_2 propellants.

The design of the HPT to be employed in the SAPERE-STRONG mission has been carried out with a combined experimental-numerical approach (Section II). Two prototypes have been developed (Section III): i) a 200 W thruster, with a target thrust of 8 mN for a 0.2 mg/s Xe mass flow rate, more suitable to preliminary testing at the CISAS facility,[14] ii) the 1 kW thruster which is the real goal of the project. The testing campaign devoted to the optimization and characterization of the thruster is ongoing at the CISAS facility; in this paper we will present only preliminary results of the 200 W prototype (Section IV), the conclusion of the testing campaign is scheduled within the next months (Section VI).

II. Methodology

We have adopted an integrated numerical-experimental approach to design and develop the thruster (see Figure 2) for the STRONG project. The experimental setup, and the numerical codes employed will be described hereinafter.

A. Experimental Characterization

The testing campaign devoted to the optimization and the characterization of the STRONG thruster is ongoing at the CISAS high vacuum facility. The thruster performances have been evaluated with both a thrust balance[15] designed within the same project and the other diagnostics available at the CISAS facility,[14,16,17] e.g. a Faraday cup. The combination of the different measurements methods have allowed to validate the new instrument (i.e. the stand), and to obtain more accurate results. The instrumentation employed is described hereinafter.

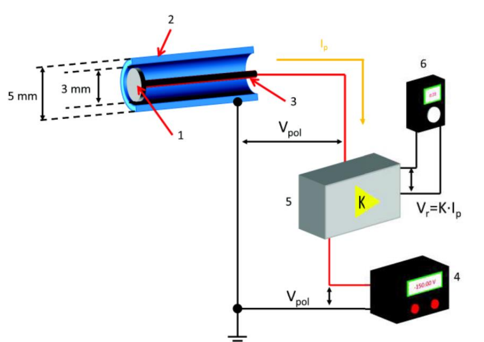

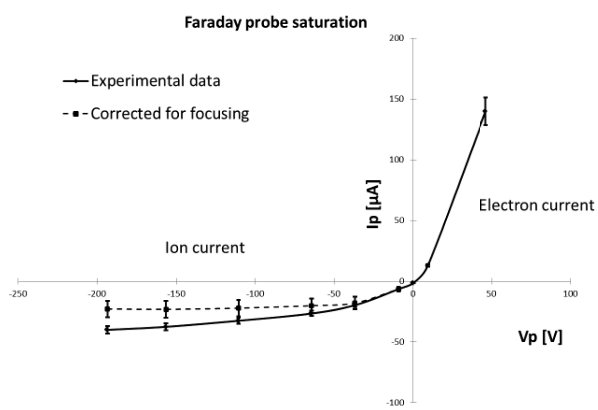

Figure 3. Faraday cup, experimental setup and saturation curve.

1. *Electrical Measurements*

We can deduce the thrust T produced by our motor and the associated specific impulse I_{sp} from the total ion current I_{ion} and the ion energyE_{ion}, in fact

$$T = \gamma \dot{m}_{ion} v_{ion} \tag{1}$$

$$I_{sp} = \gamma \eta_m v_{ion} / g_0 \tag{2}$$

where $\dot{m}_{ion}$ is the ion mass flow rate, v_{ion} is the ion speed, γ is the beam divergence factor,[14] η_m is the mass utilization efficiency, and g_0 is the Earth gravitational acceleration at the sea level. In particular $\dot{m}_{ion} = I_{ion} m_{ion}/q$, where q is the ion charge; in our case q is the elementary charge because, from spectroscopic measurements,[16] we have verified that the population of second ionized particles is negligible. Trivially the ion speed derives from ion energy $v_{ion} = \sqrt{2E_{ion}/m_{ion}}$.

Both total ion current and ion energy are measured with the Faraday cup available at CISAS facility. The probe (reported in Figure 3(a)) consists of a 3 mm polarized nickel plate collector, encased in a stainless steel cylinder which acts as a guard ring. The collector and the ring are electrically insulated; the ring is grounded, while the collector is connected to the dedicated analog conditioning and acquisition electronics which measures the incoming ion current.

The ion energy can be estimated from the Faraday cup saturation curve: "corrected" saturation ion current is never reached (see Figure 3(b)) because of an electrostatic focusing effect which, for increasingly negative polarization voltages, tends to deviate the ion trajectories towards the probe, effectively increasing its capture area. From the inclination of the "experimental ion saturated current" we can infer the ion energy.[14] Once the ion energy is known, the total ion current can be calculated by integrating the radial current density profile (corrected for the focusing effect) over the corresponding plume circular area.

2. Thrust Stand Measurements

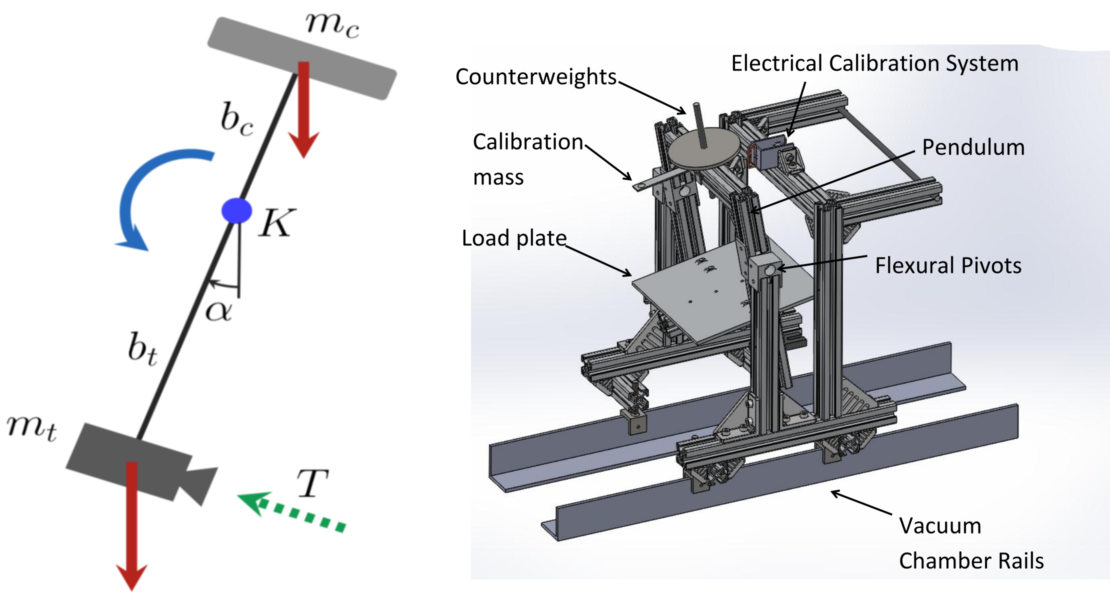

Figure 4. Scheme and CAD model of the thrust balance.

We have developed a thrust stand (see Figure 4) for RF plasma thruster characterization, capable of: i) allowing for an high number of measurements per day; ii) being high immune to RF disturbances, iii) allowing for testing thrusters of different mass, iv) being installed in the CISAS vacuum chamber. The configuration which meets best these requirements is the reconfigurable counterbalanced-type pendulum devoid of any null-displacement system. Adjusting the amount of counterweights the balance can vary its sensibility, being capable of measuring thrusts in the range from 10 μN to 100 mN. The stand can carry weights up to 5 kg.

As we can see in the scheme reported in Figure 4(a), the thrust T is related to the pendulum arm rotation angle α by means of the rotational equilibrium equation

$$K\alpha = T b_t \cos(\alpha) + g \sin(\alpha)(m_c b_c - m_t b_t) \tag{3}$$

in which b_t is the distance between the thruster and the pivot, m_t is the thruster mass, b_c is the length of the arm between the counterweights and the pivot, m_c is the counterweights mass, and K is the torsional

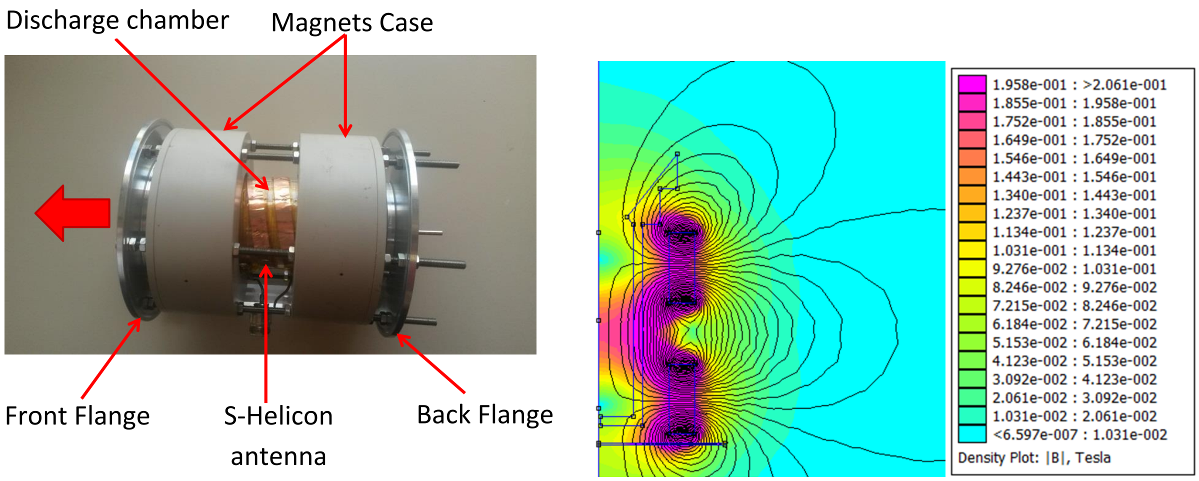

Figure 5. STRONG thruster without the lateral aluminum cover, and the magnetic field topology calculated with FEMM.

stiffness of the pivot. Rather than measuring α we measure the horizontal displacement of a fixed point in the arm.

The design of the thrust stand is reported in Figure 4(b). Commercially available components such as standard aluminum profiles have been selected in order to reduce the costs. The oscillating pendulum arm is connected to the frame by means of two Riverhawk 5020-800 flexural pivots. The thruster is fastened to a load plane integrated in the pendulum arm. The pendulum arm displacement is measured by means of an Agilent 5529A near-IR laser interferometer, which is capable of a resolution inferior to 0.01 μm. The laser is focused through a series of mirrors on a corner cube reflector, placed on the inferior tip of the rotating arm of the balance. Vibrational noise damping is provided by an eddy current brake. The principal calibration is provided by the application of calibrated masses; also a secondary electric calibration system, for verification during the test session, is present.

B. Numerical Characterization

Numerical tools have been employed for both the preliminary design and the optimization of the thruster. A global model[18] has been employed in the preliminary design phase to determine the general layout of the thruster in terms of geometry, input power, magnetic field and mass flow rate in order to achieve the desired thrust and specific impulse levels. The design was subsequently refined by means of a combined experimental-numerical approach[17,19,20] in which a reconfigurable thruster development model was employed to characterize the plasma source and collect data to benchmark the results of PIC,[21] fluid[22] and electromagnetic[23] simulation codes developed in our research group. When a sufficiently good agreement between experimental and numerical data is reached the codes can be employed for the optimization of the design.

III. Prototypes Description

During the development process we had designed and manufactured two prototypes[14,24] of the thruster: i) 1 kW prototype with a target thrust of approximately 100 mN which reproduce the dimensions of the target STRONG thruster, ii) 200 W prototype with a target thrust of 8 mN at 0.2 mg/s Xe mass flow rate, this motor is more suitable for the preliminary characterization. Both prototypes are highly reconfigurable (e.g. magnets can be moved and the antenna geometry can be easily modified) in order to maximize the number of thruster configurations that can be tested per day.

A. 1 kW prototype

In Figure 5(a) we have reported a picture of the 1 kW STRONG prototype. The plasma chamber has a cylindrical shape with an inner diameter $\phi_{in} = 40$ mm and length $L = 109$ mm. The outer diameter of the

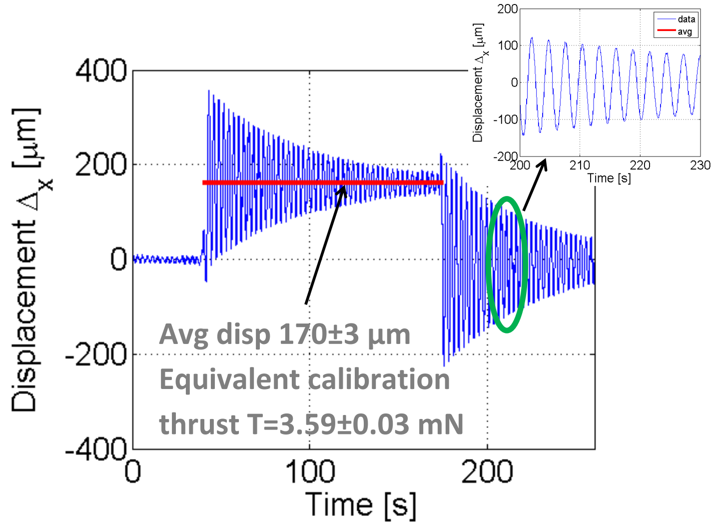

Figure 6. Calibration procedure: horizontal displacement of the balance's mobile arm in function of time. The thruster under test is the 200 W prototype. The calibration consists on the application of a calibrated mass of 0.677 ± 0.001 g which generates an equivalent thrust of 3.59 ± 0.03 mN. The sensibility of the instrument is therefore $\mathbf{R_T} = 47.4 \pm 1.2$ μm/mN. Zoom highlights the sinusoidal dumped oscillation of the balance after the mass removal.

chamber ϕ_{out} depends on the diameter of the outlet disk, which in turn is related to the diameter of the orifice. The chamber has been realized in hBN because of its relatively high thermal conduction coefficient (up to 600 W/(m K)), low density (≈2100 kg/m^3), high resistance to erosion due to plasma, and high maximum operating temperature (up to 2270 K).

Permanent magnets are devoted to the generation of the magneto-static field. Two rings of radially polarized magnets in SmCo produce a magnetic field of ≈ 1500 G within the plasma source, and a proper shaped magnetic nozzle at the source exhaust (see Figure 5(b)). This configuration of magnets, even though capable of producing an intense magnetic field in the source, is affected by the presence of two radial cusps, which however does not affect the thruster performances significantly. The magnets rings are encased in dedicated supports made in PEEK, this material has been selected because of its good mechanical properties, high temperature resistance and high thermal insulation. The thruster is encased in a radial screen of mu-metal[25] (not depicted in Figure 5) which reduces the interferences with other subsystems of the satellite. Also the back flange is screened with a thin disk of the same material; on the contrary the frontal flange is unscreened in order to maintain the proper shape of magnetic field lines in the magnetic nozzle region.

The power necessary to maintain the plasma discharge inside the source is provided by a RF antenna of the S-Helicon type wrapped around the chamber. The S-Helicon antenna concept has been developed during the HPH.COM program, and has been patented (International PCT/IB2016/050199 15.01.2016, Italian patent number VR2015A000007 del 16.01.2015).

The correct positioning of the components and the structural integrity are guaranteed by an aluminum frame composed of two flanges held together by threaded bars. The structure shown in Figure 5(a) is not complete because the thruster will be encased in a cylindrical aluminum skin fixed between the two flanges.

The overall mass of the propulsive subsystem is about 6 kg, with an overall diameter of 145 mm and a length of 162 mm. The estimated weight include the Power Processing Unit (PPU) and the Thermal Control System (TCS); the latter has been sized employing a completely passive strategy which consist of a combination of Multi-Layer Insulator (MLI) blankets, radiator panels and heat pipes.

B. 200 W prototype

The 200 W prototype has the same main features of the 1 kW thruster, the concept and the materials employed are the same. The principal difference between the two models is the size, the discharge chamber of the 200 W prototype has an inner diameter $\phi_{in} = 27$ mm and length $L = 65$ mm. The magnetic field inside the source is ≈ 1500 G as in the 1 kW model. The thruster mass is roughly 1.5 kg (without PPU and TCS), the diameter 85 mm and the length 130,5 mm.

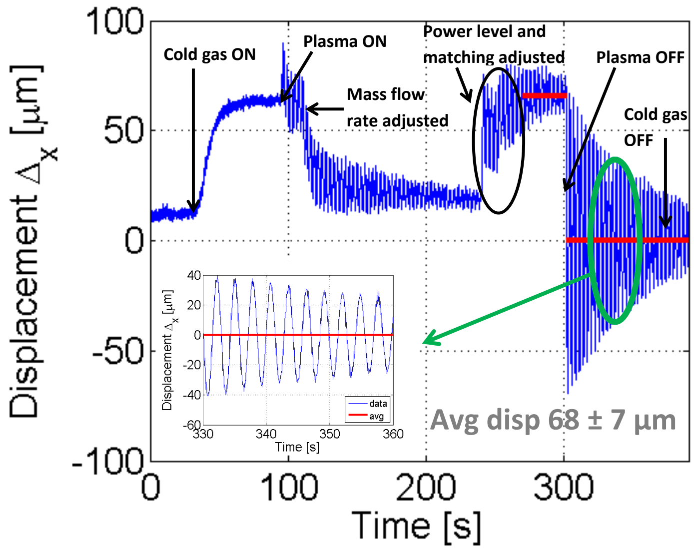

Figure 7. Thrust measurement procedure: horizontal displacement of the balance's mobile arm in function of time. The thruster under test is the 200 W prototype operated with a Xe mass flow rate of 0.2 mg/s, and an input power of 150 W. The recorded signal reports: i) supply of 1 mg Xe mass flow rate at t=30 s, ii) plasma switch on at 20 W at t=90 s, iii) mass flow rate adjusted to 0.2 mg at t=105 s, iv) power and electric matching adjusted to 150 W between t=240 s and t= 270 s, v) plasma switch off at t=300 s, vi) cold gas switch off at t=360 s. Provided that the cold gas contribution to the thrust is negligible and that the average displacement generated by the plasma switch off is 68 ± 7 μm, the measured thrust is 1.43 ± 0.18 mN in accordance with the calibration reported in Figure 6. Zoom highlights the sinusoidal dumped oscillation of the balance after the plasma switch off.

IV. Results

Provided that the optimization and testing campaign is still ongoing at the CISAS facility, here we will present only preliminary results related to the 200 W prototype. In this section we will: i) describe the thrust measurement procedure with the balance using, as example, a 150 W input power and 0.2 mg/s Xe mass flow rate test; ii) present a preliminary characterization of the thruster performances in function of the input power, in the range from 50 W up to 200 W, and mass flow rate, in the range 0.05 mg/s up to 0.4 mg/s.

A. Thrust balance measurement

In Figure 6 we have reported the calibration procedure devoted to the identification of the instrument sensibility. At $t = 40$ s we loaded the mobile arm of the pendulum with a known mass that generates the same torque of a thrust $T = 3.59 \pm 0.03$ mN; we removed the calibration mass at $t = 175$ s. The average displacement generated by the calibration mass is $\Delta_x = 170 \pm 3$ μm, therefor the instrument sensibility is $R_T = \Delta_x/T = 47.4 \pm 1.2$ μm/AU. The uncertainty calculation has been performed in accordance with ISO/IEC GUIDE 98-3:2008(E) (GUM, 1995). In the zoomed portion of Figure 6 we can see the sinusoidal dumped oscillation of the mobile arm after the mass removal.

Once the instrument sensibility is known, we can measure the thrust generated by our prototype by means of the test reported in Figure 7; the thruster is operated with Xe, the imposed mass flow rate is 0.2 mg/s and the imposed power is 150 W. The test consists in: i) at $t = 30$ s supplying a 1.0 mg/s Xe mass flow rate, ii) at $t = 90$ s switching on the plasma at a 20 W power level, iii) at $t = 105$ s regulating the mass flow rate at the nominal test value of 1.6 mg/s, iv) between $t = 240$ s and $t = 270$ s regulating the power level at 150 W and adjusting the electrical matching, v) at $t = 300$ s switching off the plasma, vi) at $t = 360$ s switching off the cold gas mass flow rate. We can notice that the cold gas switch off produced negligible variations in the mean value of the displacement, therefore we can assume that only plasma contributes to the thrust. The difference between the average value of the displacement after and before the plasma switch off is $\Delta_x = 68 \pm 7$ μm. In accordance with the calibration reported in Figure 6, the thrust produced by our motor is $T = \Delta_x/R_T = 1.43 \pm 0.18$ mN. The thrust stand measurement has an error in the range of 10% as predicted in previous works about the balance.[15] The mean position of the mobile arm of the balance is different between the beginning and the end of the test, this is due to thermal drift: the thruster mass center drifts because of thermal gradients mainly generated by plasma heat losses. In this case thermal drifts are not as evident as in other tests[15] because of the low plasma power dissipation in respect to the thruster mass. In the zoomed portion of Figure 7 we can see the sinusoidal dumped oscillation of the mobile arm after the plasma switch off.

B. Preliminary performances characterization

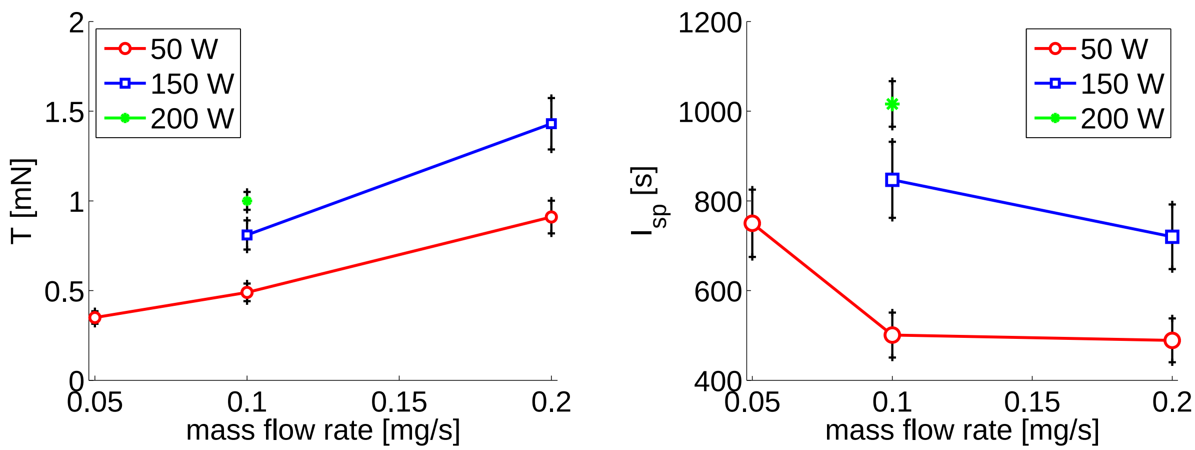

Figure 8. Preliminary performances characterization: a) thrust T in function of the Xe mass flow rate for three input power levels, b) specific impulse I_{sp} in function of the Xe mass flow rate for three input power levels. Reported the measurement mean value and the relative uncertainty.

In Figure 8 we have reported a preliminary performances characterization, the measurements have been done with the CISAS thrust stand. The Xe mass flow rate is variable in the range from 0.05 mg/s up to 0.2 mg/s, the input power range from 50 W up to 200 W. From Figure 8(a) we can see that the thrust increases with both the input power and the mass flow rate in the considered range. From Figure 8(b) we can see that the specific impulse increases with the input power and decreases with the mass flow rate. The target performance of the 200 W prototype is $T = 8$ mN with a mass flow rate of 0.4 mg/s and an input power of 200 W, and therefore a specific impulse $I_{sp} = 2000$ s. The eventual necessity of a further increase in the thruster performances will be highlighted by a characterization performed in a wider range of input power and mass flow rate.

V. Conclusions

The University of Padova is the partner of the research project SAPERE/STRONG responsible for the design, realization and testing of the HPT which will constitute the principal propulsion system of a space tug, coupled to the rocket VEGA, devoted to the transfer of payloads from intermediate orbits to the target orbit. The HPT to be realized has an input power of 1 kW, a target thrust of 100 mN, and is capable of working with Xe, Ar and CO_2 propellants. We have developed two prototypes: i) a 200 W thruster whose target performance is 8 mN with a Xe mass flow rate of 0.4 mg/s, this prototype is more suitable to preliminary testing; ii) a 1 kW thruster which is the real goal of the project. The principal instrumentation employed for the performances characterization is the combination of a thrust balance, realized within the same STRONG project, and a Faraday probe. The testing campaign devoted to the optimization and characterization of the thruster is ongoing at the CISAS facility. We have reported a measurement test, performed with our balance on the 200 W prototype, from which we have evaluated a thrust $T = 1.43 \pm 0.18$ mN for an input power of 150 W and a Xe mass flow rate of 0.2 mg/s. We have also reported the results of a preliminary performance characterization performed on the 200 W prototype with our thrust stand: the thrust increases with both power input and mass flow rate, while the specific impulse decreases with mass flow rate.

VI. Future Works

The testing campaign will conclude within the next months; we have scheduled: i) the extension of the performances characterization to a wider range of input power and mass flow rate; ii) the optimization of the thruster performances. We are confident that the performances can be further increased because the 200 W prototype tested until now is only a basic version which can be reconfigured and updated. The development strategy will be focused on the optimization of the magnetic field lines and antenna configuration. Once the performances of the 200 W prototype will be consolidated we will verify that the same optimization strategy can be adopted for the 1 kW prototype. In a future paper more details on the performances and on the definitive geometrical configuration of the developed prototypes will be provided.

References

[1] Edwards, C. H., et al., "The T5 ion propulsion assembly for drag compensation on GOCE", *Second International GOCE User Workshop* GOCE, The Geoid and Oceanography. 2004.

[2] Wallace, N., "Testing of the Qinetiq T6 thruster in support of the ESA BepiColombo mercury mission for the ESA BepiColombo mission", *4th International Spacecraft Propulsion Conference*, Vol. 555. 2004.

[3] Pavarin, D., et al., "Design of 50 W helicon plasma thruster", *31st Int. Electric Propulsion Conf.*, Ann Arbor, MI. 2009.

[4] Chen, F. F., "Helicon plasma sources", *High Density Plasma Sources*, 1995, pp. 1–75.

[5] Chen, F. F., and Arnush, D., "Generalized theory of helicon waves I. Normal modes", *Phys. Plasmas*, Vol. 4, No. 9, 1997, pp. 3411–3421.

[6] Chang Diaz, F. R., "The Vasimir", *Sci. Am.*, Vol. 283, No. 5, November 2000, pp. 90–97.

[7] Pavarin, D., et al., "Helicon Plasma Hydrazine Combined Micro Project Overview and Development Status", *Proceedings of the Space Propulsion Conference*, San Sebastian, Spain, 2010.

[8] Pavarin, D., et al., "Thruster development set-up for the helicon plasma hydrazine combined micro project", *Proceedings of the 32nd International Electric Propulsion Conference (IEPC 2011)*, Wiesbaden, Germany, 2011.

[9] Boswell, R. W., et al., "The helicon double layer thruster", *28th International Electric Propulsion Conference*, IEPC 2003.

[10] Batishchev, O. V., "Mini-helicon plasma thruster", *IEEE Transactions on Plasma Science*, Vol. 37, No. 8, 2009, pp.1563–1571.

[11] Shinohara, S., et al., "Development of electrodeless plasma thrusters with high-density helicon plasma sources", *IEEE Transactions on Plasma Science*, Vol. 42, No. 5, 2014, pp. 1245–1254.

[12] Merino, M., et al., "Design and development of a 1 kW-class helicon antenna thruster", *Proceedings of the 34th International Electric Propulsion Conference (IEPC 2015)*, Fairview Park, OH, 2015, IEPC-2015-297.

[13] Official CTNA web site, http://www.ctna.it/projects/

[14] Trezzolani, F., "Optimization and Automatic Control of Radio-Frequency Plasma Thrusters for Space Applications", *paduaresearch.cab.unipd.it*, PhD thesis (2015).

[15] Trezzolani, F., et al., "Development of a Counterbalanced Pendulum Thrust Stand for Electric Propulsion", *Metrology for Aerospace (MetroAeroSpace), 2017* IEEE Padova 2017.

[16] Pavarin, D., et al., "Thruster Development Set-up for the Helicon Plasma Hydrazine Combined Micro Research Project", *32th International Electric Propulsion Conference*, 11th-15th September 2011, Wiesbaden, Germany.

[17] Trezzolani, F., et al., "Integrated Design Tools for RF Antennas for Helicon Plasma Thrusters", *50th AIAA/ASME/SAE/ASEE Joint Propulsion Conference.*

[18] Manente, M., et al., "Numerical simulation of the Helicon double layer thruster concept", *AIAA Paper* 2007-5312, 2007.

[19] Bosi, F. J., et al., "Modeling and optimization of electrode-less helicon plasma thruster with different propellants", *50th AIAA/ASME/SAE/ASEE Joint Propulsion Conference*, Cleveland, USA, 2014.

[20] Melazzi, D., et al., "Plasma Source Optimization for Multispecies Helicon Plasma Thruster", *50th AIAA/ASME/SAE/ASEE Joint Propulsion Conference*, Cleveland, USA, 2014.

[21] Pavarin, D., et al., "Development of Plasma Codes for the Design of Mini-Helicon Thrusters", *32nd International Electric Propulsion Conference*, IEPC 2011.

[22] Magarotto, M., et al., "Numerical Model of an Helicon Plasma Source for Space Propulsion Application" *European Conference for Aerospace Sciences*, EUCASS 2017.

[23] Melazzi, D., and V. Lancellotti. "ADAMANT: A surface and volume integral-equation solver for the analysis and design of Helicon plasma sources", *Computer Physics Communications*, Vol. 185, No. 7, 2014, pp. 1914–1925.

[24] Trezzolani, F., et al., "Experimental characterization of a kW-level radio-frequency plasma thruster for project SAPERE-STRONG", *proceedings of the Space Propulsion Conference*, Rome, Italy, 2016.

[25] Official MμShield®web site: http://www.mumetal.com